Poster No.2: Modification and application of virtual submesh cellular automata method in additive manufacturing

Ling Shi[1], Songzhe Xu[1,*], Jingjing Li[1], Heyu Lu[1], Chaoyue Chen[1], Jiang Wang[1,*], Zhongming Ren[1]

[1]Shanghai University, Shanghai, China

Email addresses: songzhex@shu.edu.cn (Songzhe Xu), jiangwang@i.shu.edu.cn (Jiang Wang)

Abstract

The cellular automata (CA) method has been widely used in microstructure simulation during solidification. A novel high-efficiency virtual submesh cellular automata (VISCA) method is proposed to reduce the mesh-induced artificial anisotropy. This method conceptually divides the mesh into a series of submeshes by giving a unique index to each CA cell. The proposed VISCA method results in a good accuracy in all orientations using uniform mesh, while an aggressive time stepping can be used. The nucleation is simulated based on a continuous nucleation model, and the Kurz-Giovanola-Trivedi (KGT) model is used to simulate the growth of the grains nucleated in the bulk material. For the application of single crystal additive manufacturing, a Single-Crystal-Texture cellular automata (SITCA) method are developed based on VISCA method to predict the nucleation and growth direction in molten pool. Besides the orientation of grain, a random number is introduced in the SITCA method to distinguish the regions of same crystallographic orientation but different growth direction in molten pool. The re-melting experiments are implemented by a top flat laser source on a Ni-based superalloy SX substrate. The heat history of the substrate boundary is measured by several thermocouples to generated the boundary condition of heat transfer simulation. The molten pool width, depth and the stray grain location of simulation are compared to experiments.

KEY WORDS: Cellular automata method; nickel-based superalloy; direct energy deposition; single crystal;

Model description

VISCA method

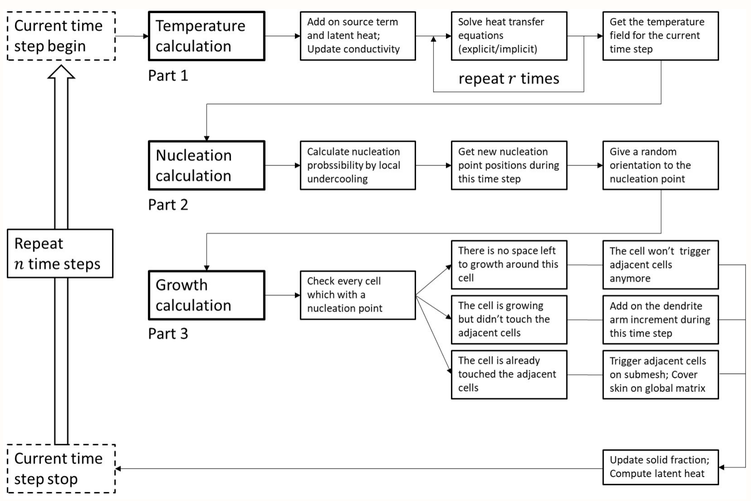

Figure 1: Procedure of the VISCA method.

The mainly procedure of VISCA method is shown in fig.1. The calculation procedure for each time step consists of three parts: heat diffusion calculation, nucleation calculation, and grain growth calculation. At the beginning of a time step, the heat transfer process is solved by explicit/implicit finite difference method (depending on the space/time scale). The second part is the nucleation calculation. The nucleation probability of each cell in the global mesh can be derived (probability equation are described in our previous work [1]) through the local undercooling ΔT. After rolling a random number, the new nucleation cell in the liquid at the current time step is selected with a random orientation Θ. Then, a virtual submesh (shown in fig.2) with the same orientation is constructed around the nucleated cell. The third part is the crystal growth calculation. Based on the previous work [2, 3], the grain growth process is reproduced by integrate the dendrite tip velocity (calculated by KGT model [4]) at current time step to the primary dendrite length. As is shown in fig.2, the growth process is operated on the submesh. If the primary dendrite length of a cell (on submesh) exceed the submesh step length, the adjacent cells of the cell will be activated to growth.

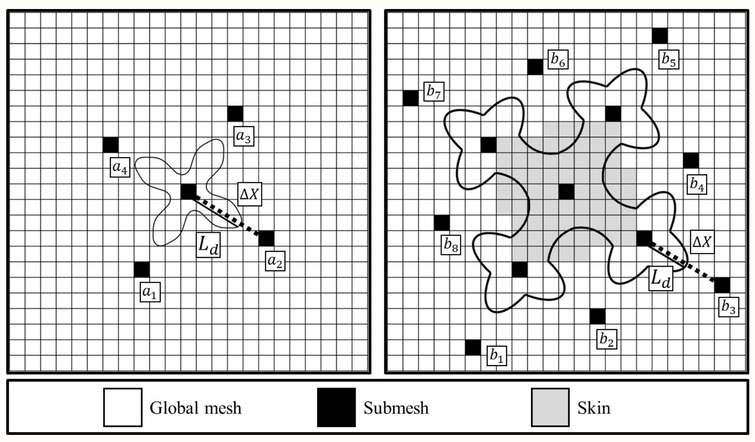

Figure 2: schematic diagram of grain growth on submesh in VISCA method.

SITCA method

The traditional cellular method with the grain envelope simplification usually ignore the dendrite branching behaviour and the crystal orientation evolution in computational area is simulated to investigate the grain distribution. As for the single crystal (SX) fabrication, not only the uniform crystal orientation is necessary, but also the uniform crystal growth direction. To reproduce the growth competition between different primary dendrite direction (not the crystal orientation), a modified cellular automata method, the Single-Crystal-Texture-Cellular-Automata method (SITCA) is developed. Besides the orientation Θ, a random number ξ, is introduced to reproduce the epitaxial growth process. As is shown in fig.3, for the crystal growth around existing SX boundary in liquid, the random number ξ, distribution texture meaning the primary dendrite growth direction.

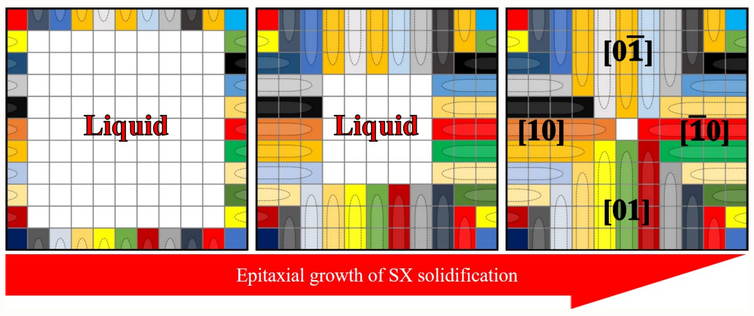

Figure 3: schematic diagram of epitaxial growth in SITCA method.

To predict the epitaxial growth situation of additive manufacturing on a SX substrate, a finite element method (FEM) model is coupled with SITCA model. To compared to the SX additive manufacturing experiments (laser remelting process on René N5 SX substrate), the FEM model of convective heat transfer is set up to calculate the temperature field. As is shown in fig.4, the temperature information on FEM encrypted unstructured grid is interpolated to SITCA mesh by shape function on nodes of each element.

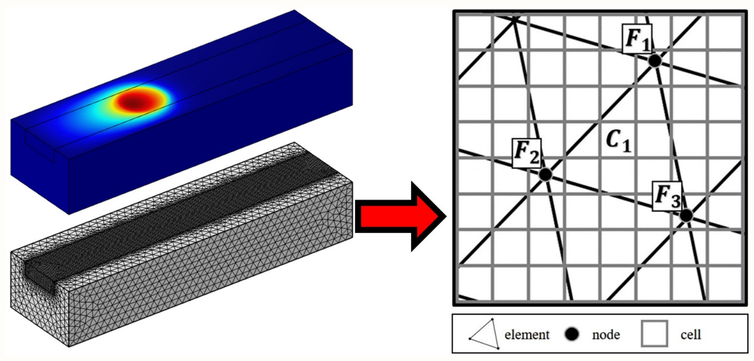

Figure 4: schematic diagram of interpolation from FEM grid to CA mesh.

Result and discussions

Validation of FEM model

As is shown in fig.5, the FEM model is compared to experimental observed molten pool width and depth. Due to the randomness of SX substrate, the temperature field is calibrated by experimental observed molten pool boundary. The validated FEM thermal field is coupled to SITCA model.

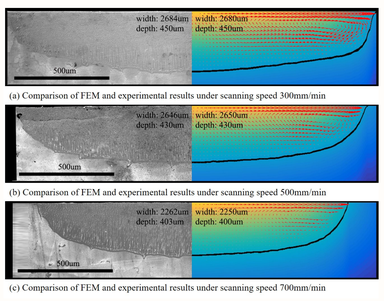

Figure 5: Comparison of molten pool dimensions between experiments and FEM model.

Validation of SITCA model

Based on the validated and interpolated thermal field, the single crystal texture and columnar to equiaxed transition (CET) in molten pool are simulated via SITCA model. To validate the SITCA model, the mathematical model [5, 6] results and experimental results are compared to the SITCA simulation results. The relative height of [001] growth direction (Ratio of [001] height to molten pool depth) is chosen to quantitatively evaluate epitaxial growth of SX substrate.

As is shown in fig.6, the mathematical model calculated and SITCA simulated relative [001] height are 31% under a laser scanning speed $300\mathrm{mm/min}$. But for scanning speed $500\mathrm{mm/min}$, the SITCA simulated [001] height is 50% and the mathematical model calculated one is 46%. The corresponding experimental results are shown in fig.7. The experimental observed relative [001] height of $300\mathrm{mm/min}$ is 30% when the one of $500\mathrm{mm/min}$ is 50%. The SITCA simulation results is obviously closer to the experiments results.

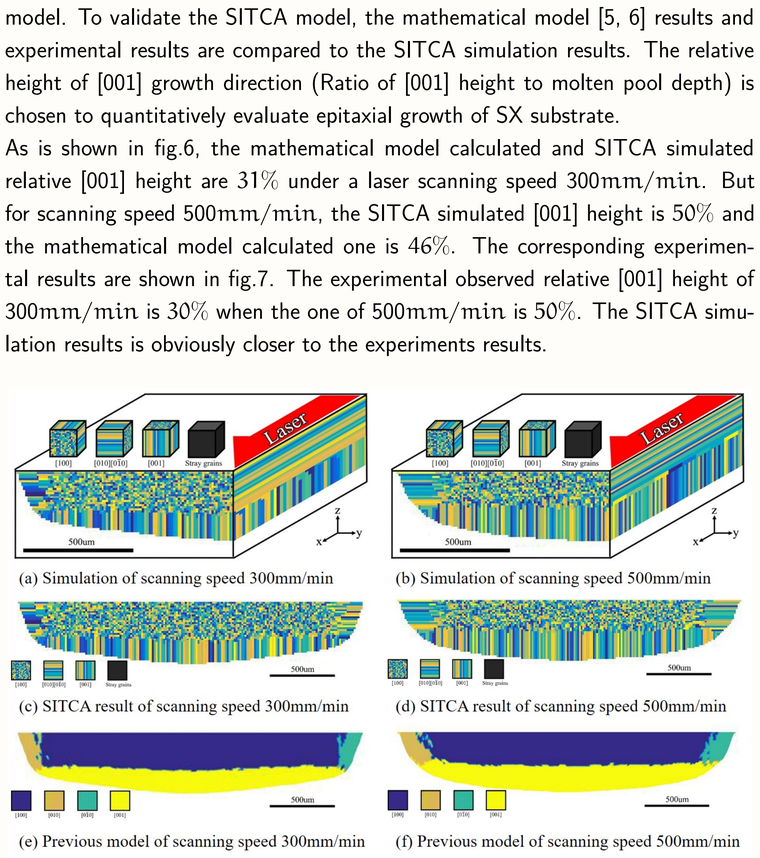

Figure 6: Comparison between simulation and mathematical model in epitaxial growth (scanning speed of $300/500\mathrm{mm/min}$).

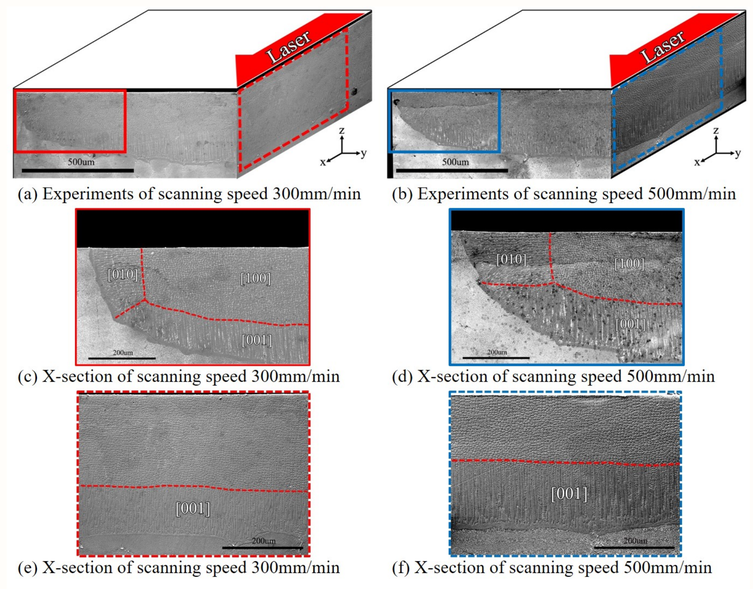

Figure 7: Experimental observation of epitaxial growth (scanning speed of $300/500\mathrm{mm/min}$).

Based on the experimental and simulation results, the relative [001] height is higher with a higher laser scanning speed. To further improve the [001] height, the experiment, simulation and mathematical model calculation of scanning speed $700\mathrm{mm/min}$ are implemented (shown in fig.8). The experimental observed relative [001] height is 64%. The simulated one is 55% and the model calculated one is 51%. The SITCA model also successful predict the generation of stray grains. All the experimental, simulated and calculated results are summarised in table.1.

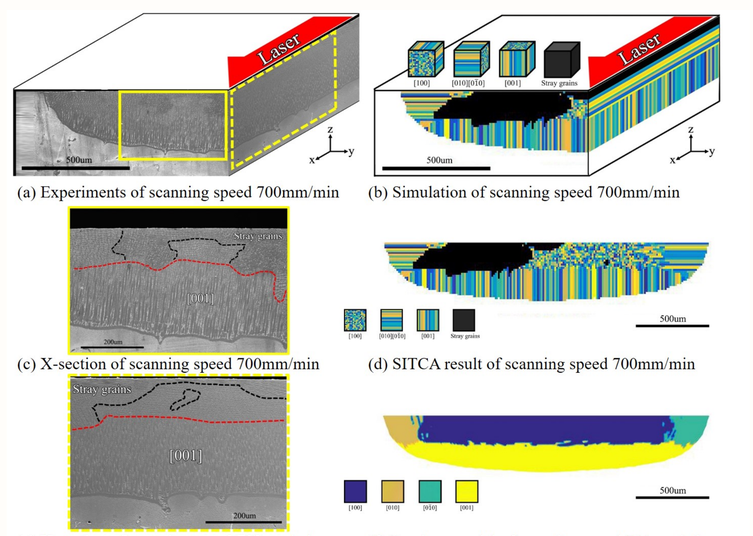

Figure 8: Comparison among experiment, simulation and mathematical model in epitaxial growth (scanning speed of $700\mathrm{mm/min}$).

Table 1: Comparison of simulated, mathematical model and experimental observed epitaxial growth.

Laser speed		Experiment	Simulation	Mathematical model
$300\mathrm{mm/min}$	[001] height	31%	30%	30%
	CET	No	No	Yes
$500\mathrm{mm/min}$	[001] height	50%	50%	46%
	CET	No	No	Yes
$700\mathrm{mm/min}$	[001] height	66%	55%	51%
	CET	Yes	Yes	Yes

Summary and conclusions

1. Based on the modification of the previous CA method [1], the SITCA model is able to reproduce not only the crystal orientation, but also the growth direction. The SITCA model can simulate in a larger scale with fewer meshes compared to model for dendrite growth simulation.
2. For the introduction of KGT model [4], the SITCA model reproduce the solid-liquid interface more realistically. Compared with the previous mathematical model, the SITCA simulation results are in better agreement with the experimental observation results in terms of [001] growth direction height and stray grains distribution, especially in the situation of high laser scanning speed.
3. Based on the experimental results, simulation results and analysis above, a higher scanning speed lead to a higher relative height of [001] direction, but more stray grains in the upper part of molten pool. The laser scanning speed should be chosen carefully to balance these two factors.

References

[1] L. Shi, S. Xu, H. Lu, C. Chen, S. Shuai, T. Hu, A. Kao, J. Wang, and Z. Ren, "A high-efficiency virtual submesh cellular automata method for solidification simulation with low mesh anisotropy," *ISIJ International*, vol. 62, no. 8, pp. 1674–1683, 2022.

[2] M. Rappaz and C.-A. Gandin, "Probabilistic modelling of microstructure formation in solidification processes," *Acta metallurgica et materialia*, vol. 41, no. 2, pp. 345–360, 1993.

[3] O. Zinovieva, A. Zinoviev, V. Ploshikhin, V. Romanova, and R. Balokhonov, "A solution to the problem of the mesh anisotropy in cellular automata simulations of grain growth," *Computational Materials Science*, vol. 108, pp. 168–176, 2015.

[4] W. . Kurz, B. Giovanola, and R. Trivedi, "Theory of microstructural development during rapid solidification," *Acta metallurgica*, vol. 34, no. 5, pp. 823–830, 1986.

[5] Z. Liu and H. Qi, "Effects of processing parameters on crystal growth and microstructure formation in laser powder deposition of single-crystal superalloy," *Journal of Materials Processing Technology*, vol. 216, pp. 19–27, 2015.

[6] Z. Liu and H. Qi, "Effects of substrate crystallographic orientations on crystal growth and microstructure formation in laser powder deposition of nickel-based superalloy," *Acta Materialia*, vol. 87, pp. 248–258, 2015.